

This discussion paper is/has been under review for the journal Atmospheric Chemistry and Physics (ACP). Please refer to the corresponding final paper in ACP if available.

Long-term in situ measurements of NO_x and NO_y at Jungfraujoch 1998–2009: time series analysis and evaluation¹

S. Pandey Deolal¹, D. Brunner², M. Steinbacher², U. Weers¹, and J. Staehelin¹

¹Institute for Atmospheric and Climate Science, Swiss Federal Institute of Technology, Zürich, Switzerland

²Empa, Swiss Federal Laboratories for Materials Science and Technology, Dübendorf, Switzerland

Received: 2 July 2011 – Accepted: 23 July 2011 – Published: 4 August 2011

Correspondence to: S. Pandey Deolal (shubha.pandey@env.ethz.ch)

Published by Copernicus Publications on behalf of the European Geosciences Union.

ACPD

11, 21835–21875, 2011

Discussion Paper | Discussion Paper

Long-term in situ measurements of NO_x and NO_y at Jungfraujoch

S. Pandey Deolal et al.

[Title Page](#)

[Abstract](#)

[Introduction](#)

[Conclusions](#)

[References](#)

[Tables](#)

[Figures](#)

◀

▶

◀

▶

[Back](#)

[Close](#)

[Full Screen / Esc](#)

[Printer-friendly Version](#)

[Interactive Discussion](#)



We present an analysis of the NO_y (NO_x + other oxidized species) measurements at the high alpine site Jungfraujoch (JFJ, 3580 m a.s.l.) for the period 1998–2009, which is the longest continuous NO_y data set reported from the lower free troposphere worldwide. Due to stringent emission control regulations, nitrogen oxides (NO_x) emissions have been reduced significantly in Europe since the late 1980s as well as during the investigation period. However, the time series of NO_y at JFJ does not show a consistent trend but a maximum during 2002 to 2004 and a decreasing tendency thereafter. The seasonal cycle of NO_y exhibits a maximum in the warm season and a minimum in the cold months, opposite to measurements in the PBL, reflecting the seasonal changes in vertical transport and mixing. Except for summer, the seasonal mean NO_x concentrations at JFJ show a high year-to-year variability which is strongly controlled by short episodic pollution events obscuring any long-term trends. The low variability in mean and median NO_x values in summer is quite remarkable indicating rapid photochemical conversion of NO_x to higher oxidized species (NO_z) of the NO_y family on a timescale shorter than the time required to transport polluted air from the boundary layer to JFJ. In order to evaluate the quality of the NO_y data series, an in-situ intercomparison with a second collocated NO_y analyzer with a separate inlet was performed in 2009–2010 which showed an agreement within 10 % including all uncertainties and errors.

20 1 Introduction

Nitrogen oxides (NO_x : the sum of nitrogen monoxide (NO) and nitrogen dioxide (NO_2)) in the troposphere are important precursors for tropospheric ozone and also influence the hydroxyl and peroxy radical concentrations which govern the life time of various gases in the troposphere (Levy, 1971; Logan, 1981; Wennberg et al., 1998). In the troposphere, nitrogen species are primarily emitted in the form of NO_x from anthropogenic sources and are subsequently oxidized to other reactive nitrogen species

Long-term in situ measurements of NO_x and NO_y at Jungfraujoch

S. Pandey Deolal et al.

[Title Page](#)[Abstract](#)[Introduction](#)[Conclusions](#)[References](#)[Tables](#)[Figures](#)[◀](#)[▶](#)[◀](#)[▶](#)[Back](#)[Close](#)[Full Screen / Esc](#)[Printer-friendly Version](#)[Interactive Discussion](#)

along a number of different pathways (Fahey et al., 1986). The complete family of reactive nitrogen species is denoted as NO_y which includes the sum of NO_x and its oxidation products (Logan, 1983):



5 In order to obtain a better understanding of tropospheric chemistry, it is therefore essential to quantify the abundance of NO_y species and their changes with time using long-term observations. Such data may serve as an important input to test models (Fahey et al., 1985; Hayden et al., 2003). Tropospheric NO_y measurements from numerous campaigns were compiled in the period 1985–1995 by Thakur et al. (1999)

10 and Emmons et al. (1997) to evaluate tropospheric chemistry transport models for estimating the global distribution of nitrogen species. Both studies indicated differences between the model and observations and the limited spatial and temporal coverage of NO_y measurements made it difficult to get reliable estimates from these simulations. Several studies in the past have examined NO_y as well as individual reactive nitrogen

15 species in different environments from aircraft measurements or ground observations (Fahey et al., 1986; Singh et al., 1992a, b; Williams et al., 1997; Brunner et al., 1998; Harrison et al., 1999; Levy et al., 1999; Zellweger et al., 2000; Thornberry et al., 2001; Stohl et al., 2002; Day et al., 2003; Hegglin et al., 2006). However, long-term trend evaluations of NO_y measurements have not been addressed so far due to the very limited availability of data sets as these measurements require frequent maintenance.

20

In Switzerland and other European countries, the NO_x emissions were reduced significantly in the early 1990's due to the implementation of catalytic converters in vehicles and other emission reduction measures. In view of this, a decreasing trend would be expected in NO_y concentrations measured at European sites. Some mountainous sites in Europe (Jungfraujoch, Hohenpeissenberg, Zugspitze and Sonnblick) have started continuous measurements of NO_y in the late 1990's as a part of the Global Atmospheric Watch (GAW) program but a trend analysis of these data has been missing so far. European trends in other trace gases such as CO , O_3 , NO_2 and NO_x from Europe, in contrast, have been addressed in many previous studies (Zanis et al., 1999;

Long-term in situ measurements of NO_x and NO_y at Jungfraujoch

S. Pandey Deolal et al.

[Title Page](#)

[Abstract](#)

[Introduction](#)

[Conclusions](#)

[References](#)

[Tables](#)

[Figures](#)

◀

▶

[Back](#)

[Close](#)

[Full Screen / Esc](#)

[Printer-friendly Version](#)

[Interactive Discussion](#)



Bronnimann et al., 2000; Derwent et al., 2003; Kaiser et al., 2007; Ordóñez et al., 2007; Gilge et al., 2010). In this context, the measurements of Jungfraujoch provide a unique opportunity to analyze the evolution of NO_y above Europe, mostly representative of the free troposphere. NO_y has been continuously measured at Jungfraujoch since 1998 by Empa. A preliminary multi-year analysis of this data set was presented by Zanis et al. (2007) for the period 1998–2004. They identified a seasonality in NO_y with a peak in April (Zanis et al., 2007) but did not perform any detailed trend analysis. Therefore, in the present study, we provide the first long-term (1998–2009) assessment of NO_y concentrations above Europe. To our knowledge, this data set is the longest continuous 10 series of NO_y measurements available for the free troposphere.

An important question is the reliability and long-term stability of the NO_y data record. A first evaluation of the NO_y measurements of Jungfraujoch was performed in spring 1998 with an instrument constructed by the University of East Anglia which showed that the agreement between these two measurements was within 10 % with slightly lower 15 values observed for the Empa's NO_y instrument (Carpenter et al., 2000). It was speculated that HNO_3 losses in the inlet system could be responsible for the differences (Zellweger et al., 2003). In the second part of this paper we report on a new measurement campaign performed in 2009/2010 using another NO_y instrument connected to a separate inlet designed to minimize potential HNO_3 losses. Finally, the third part of the 20 paper discusses possible local influences on the data record which may arise from the operation of the touristic infrastructure at Jungfraujoch.

2 Method and instrumentation

Measurement site: the high alpine research station Jungfraujoch (JFJ) (Sphinx observatory, 46.55°N , 7.98°E , 3580 m a.s.l.) is located in the Swiss Alps between the Mönch and the Jungfrau mountain peaks. It is one of the currently 28 global sites of the Global 25 Atmosphere Watch (GAW) program of the World Meteorological Organization (WMO). The JFJ site is also incorporated in the Swiss National Air Pollution Monitoring Network

[Title Page](#)[Abstract](#)[Introduction](#)[Conclusions](#)[References](#)[Tables](#)[Figures](#)[◀](#)[▶](#)[◀](#)[▶](#)[Back](#)[Close](#)[Full Screen / Esc](#)[Printer-friendly Version](#)[Interactive Discussion](#)

(NABEL), which is operated by the Swiss Federal Laboratories for Materials Science and Technology (Empa) in association with the Swiss Federal Office for the Environment (FOEN). The site mainly resides in the free troposphere in the autumn and winter season, while in late spring and summer it is often influenced by the planetary boundary layer (PBL) (Baltensperger et al., 1997; Lugauer et al., 1998; Zellweger et al., 2003). Long term continuous in-situ monitoring of trace gases such as NO, NO₂, NO_y, CO, and O₃ is routinely performed by Empa.

2.1 NO/NO_x/NO_y instrumentation of Empa

NABEL gas sampling system: ambient air for the different NABEL instruments is drawn into the Sphinx laboratory at a high flow rate of 50 m³ h⁻¹ through a common heated stainless steel inlet (inner diameter 90 mm, residence time about 1 s) maintained at a temperature of 10 °C. In order to minimize NO_y losses in the sampling lines, the NO_y converter is placed as close as possible to the main inlet, connected with about 1 m of PFA tubing (inner diameter 3/16", 1 l min⁻¹ flow rate, resulting residence time about 15 1 s). Thus the total residence time till the air reaches the NO_y converter is about 2 s. The photolytic converter for the NO₂ measurement is placed next to the NO_y converter. Downstream of the converter the air is drawn through separate PFA tubing to the NO analyzer. The air for the NO analysis is drawn directly from the main manifold with PFA tubing. A detailed schematic of the trace gas inlet at JFJ is shown in Fig. 1.

Instrumentation: NO, NO_x and NO_y measurements are performed by a commercial instrument (CraNOx, Eco Physics, Switzerland) having initially two and recently three chemiluminescence detectors (CLD) with temperature-controlled reaction chambers. Instrumental changes during the measurement period are provided in the Table 1. NO_y species are converted to NO on a heated gold catalyst (300 °C) in the presence of 2 % CO (purity 99.997 %, Messer-Griesheim GmbH) as a reducing agent (Fahey et al., 1985). NO_x is measured as NO after photolytic conversion of NO₂ (PLC 760 till December 2000; since then PLC 762). As mentioned above, the gold converter is mounted inside the laboratory near the NABEL sampling inlet. A CLD measurement cycle takes

[Title Page](#)[Abstract](#)[Introduction](#)[Conclusions](#)[References](#)[Tables](#)[Figures](#)[◀](#)[▶](#)[◀](#)[▶](#)[Back](#)[Close](#)[Full Screen / Esc](#)[Printer-friendly Version](#)[Interactive Discussion](#)

one minute, which includes the detection of a background signal in the pre-reaction chamber for 30 s, followed by the measurement of the sample in the main chamber for 30 s. Automated calibrations are performed every 35 h. The chemiluminescence detectors are calibrated with NO standards (about 5.0 ppm; referenced against NIST Standard Reference Material (SRM 2629a) and NMI Primary Reference Material (PRM BD11)) diluted with synthetic air to a concentration of about 45 ppb. The conversion efficiencies of the gold and photolytic converters are measured every 70 h by generating a known amount of NO_2 by gas phase titration of NO with ozone. The efficiency of the gold converter mostly ranged between 95–100 % and the efficiency of the photolytic converter ranged from 45 to 62 %. The detection limits of the CLD 770 s (30 min averages) for the NO and NO_y measurements are 20 ppt whereas it is 50 ppt for the NO_2 channel due to the incomplete conversion and the determination of NO_2 by the difference of two measured (NO and NO + converted NO_2) signals. The respective numbers for the CLD 89 p analyzers are 15 ppt (NO and NO_y) and 25 ppt (NO_2). The overall measurement uncertainty for NO_y was 9 % and 5 % for NO_x . The temporal resolution of these measurements was 2 min. Data are usually stored and processed as 10-min averages.

2.2 NO/ NO_y instrument of ETH Zurich (ETHZ)

Campaign inlet: the main objective of the campaign measurements was to evaluate the Empa instrument using an independent measurement system with a separate inlet. The inlet was mounted on the same rooftop ~4 m away from the NABEL inlet and ~10 m above the touristic platform on the northeastward facing side. Different from the Empa system the NO_y converter was mounted externally, integrated into the inlet system, to avoid any wall losses of HNO_3 . In order to protect the measurements from snow and rain, the gold converter was placed in an aluminum box (117 × 27 × 30 cm) and air was sampled through a short (~20 cm) Teflon tubing heated to about 25 °C. The sampling tubings for NO_y and NO were protected against snow and rain with a Teflon

Long-term in situ measurements of NO_x and NO_y at Jungfraujoch

S. Pandey Deolal et al.

[Title Page](#)

[Abstract](#)

[Introduction](#)

[Conclusions](#)

[References](#)

[Tables](#)

[Figures](#)

◀

▶

◀

▶

[Back](#)

[Close](#)

[Full Screen / Esc](#)

[Printer-friendly Version](#)

[Interactive Discussion](#)



hood of about 25 cm. The sampling flow rate was 1 l for both channels. A detailed schematic is given in Fig. 2.

Instrumentation: NO and NO_y measurements were performed using a highly sensitive analyzer CLD 790 SR from Eco Physics. The instrument has three chemiluminescence detectors to measure NO_y, NO and O₃ simultaneously. The NO_y converter, designed and built by the Max Planck Institute for Chemistry in Mainz, Germany (Lange et al., 2002) is a 72 cm long gold tube with an inner diameter of 5 mm. It was heated to 120 °C at the tip and 300 °C near the centre. NO_y species are catalytically converted to NO on the heated gold surface in the presence of CO acting as a reducing agent (Bollinger et al., 1983; Fahey et al., 1985). NO is subsequently measured by the CLD by detecting the chemiluminescence generated in the reaction of NO with excess ozone produced by an ozone generator from pure oxygen. CO was passed through a charcoal filter in order to reduce impurities and corresponding chemiluminescence signals in the chamber. Pure CO was added to the sample air at a flow rate of 5 sccm providing a mixing ratio of 0.5 %. The instrument was originally designed for airborne use. It was operated in several flight campaigns (Hegglin et al., 2006) and evaluated against the NO_y analyzer installed on a commercial airliner in the project MOZAIC (Pätz et al., 2006). Here, it was used for the first time for continuous measurements at the ground which required a number of modifications to allow for unattended operation during several days to weeks. To account for the signal from interfering species and the overall background chemiluminescence and photomultiplier dark current signals, the NO and NO_y measurements were operated in two different modes: main chamber and pre-chamber (Drummond et al., 1985). Measurements were performed quasi-continuously in main chamber (measurement) mode switching only every 280 s for 10 s to pre-chamber (background detection) mode.

Automatic three-stage calibrations were performed every morning between 02:00–03:00 a.m. by measuring synthetic air, NO, and gas phase titration (GPT) to determine the conversion efficiency. A pure air generator (PAG, Eco Physics, Switzerland) was used to generate zero air and a calibration unit (Multigas Calibrator S-100, Environics,

Long-term in situ measurements of NO_x and NO_y at Jungfraujoch

S. Pandey Deolal et al.

[Title Page](#)

[Abstract](#)

[Introduction](#)

[Conclusions](#)

[References](#)

[Tables](#)

[Figures](#)

◀

▶

[Back](#)

[Close](#)

[Full Screen / Esc](#)

[Printer-friendly Version](#)

[Interactive Discussion](#)

Long-term in situ measurements of NO_x and NO_y at Jungfraujoch

S. Pandey Deolal et al.

[Title Page](#)

[Abstract](#)

[Introduction](#)

[Conclusions](#)

[References](#)

[Tables](#)

[Figures](#)

[◀](#)

[▶](#)

[◀](#)

[▶](#)

[Back](#)

[Close](#)

[Full Screen / Esc](#)

[Printer-friendly Version](#)

[Interactive Discussion](#)



USA) was used to dilute the NO calibration gas and to generate the NO_2 used for the GPT by adding O_3 generated internally in the S-100 to the NO calibration gas. The NO calibration gas was taken from a reference gas cylinder (5.0 ± 0.02 ppm purity 99.99 %, Messer-Griesheim GmbH) and diluted with synthetic air to generate an output concentration of 40 ppb. In order to avoid potential differences in the calibration scale, the NO standards used by ETHZ were compared against Empa's NO standard and the reference concentrations were corrected accordingly. Nighttime NO measurements were used to test the background values since at night NO is expected to vanish in the absence of local sources due to titration by ozone. GPT calibrations were used to

5 determine the converter efficiency assuming that the conversion efficiency determined for NO_2 is representative for all NO_y species. NO_2 calibration gas generated in the S-100 by the reaction of NO with O_3 and diluted with synthetic air was added a few centimeters upstream of the NO_y converter. During the campaign, the converter had to be cleaned regularly by scrubbing with soft brushes rinsed with acetone and dis-
10 tillied water because it was observed that the conversion efficiency sometimes dropped quite rapidly. In this way, the efficiency was maintained above 90 % for most of the time (Fig. 3). The detection limit ($\pm 1\sigma$) measured for the NO and NO_y channel was 10 pptv for a time resolution of one second.

3 Results and discussion

20 3.1 Long term changes at Jungfraujoch from 1998–2009

The long-term measurements of NO_y , NO_x and NO are presented in Fig. 4 which shows monthly median values from January 1998–December 2009. NO_y data series (black) shows high interannual variability with a slight increase during the years 2002–2004. 2003 was recorded the hottest year in European history with an exception-
25 al prolonged heat wave in summer (Luterbacher et al., 2004; Schär et al., 2004, 2008) also leading to enhanced ozone levels across Europe (Fiala et al., 2003). The

Long-term in situ measurements of NO_x and NO_y at Jungfraujoch

S. Pandey Deolal et al.

[Title Page](#)[Abstract](#)[Introduction](#)[Conclusions](#)[References](#)[Tables](#)[Figures](#)[◀](#)[▶](#)[◀](#)[▶](#)[Back](#)[Close](#)[Full Screen / Esc](#)[Printer-friendly Version](#)[Interactive Discussion](#)

overall annual averages of O₃ and NO_y were highest in 2003. In addition to the trend over the whole period we therefore calculated linear trends (thick black lines) based on the monthly median values before and after 2003. From 1998–2002 the trend in NO_y was positive but not significant while from 2004–2009 a significant decreasing

5 tendency was observed at a rate of $-0.048 \pm 0.012 \text{ ppb yr}^{-1}$ (significant at the 95 % confidence level). Considering the complete NO_y time series 1998–2009 there is no significant trend (green line). The NO_x data series (blue) does not show any trend either but a rather large monthly variability. Figure 5 shows the monthly anomalies of NO_y and NO_x, determined by subtracting the mean seasonal cycle. The largest positive 10 NO_y anomaly was observed in 2002 and 2003 while in NO_x the anomaly in 2003 was comparatively small. The mean and median seasonal cycles of NO_y (black) and NO_x (blue) are additionally shown in the right hand panel in Fig. 5. NO_y measurements show a broad spring and summer maximum while NO_x shows a minimum during these months. Since the NO_x lifetime is much shorter in summer than in winter (Schaub et 15 al., 2007), NO_x concentrations at JFJ are higher in the cold season. In contrast to NO_y and NO_x, the CO measurements at JFJ exhibit a steady decrease from 1996–2007 at a rate of $-2.65 \pm 0.04 \text{ ppb yr}^{-1}$ based on background concentrations filtered for pollution events (Zellweger et al., 2009). The steady decline in CO concentrations is likely an effect of emission abatement strategies in Europe, CO concentrations in early years 20 are additionally affected by the influences of intense global biomass burning in 1998 and 2003 (Simmonds et al., 2005; Yurganov et al., 2005a) and the El-Nino event in 1998 (Koumoutsaris et al., 2008). The ozone concentrations at JFJ had a significant positive trend at Jungfraujoch in the 1990s (Ordóñez et al., 2007) and a negative but insignificant trend for the period 2000–2008 (Cui et al., 2011).

25 NO_x measurements from other NABEL stations in Switzerland from 1998–2009 for urban-suburban, rural and elevated sites (1000–1600 a.m.s.l.) is presented in Fig. 6 which show a significant decrease in NO_x at urban-suburban sites (BAFU, 2010). Elevated sites do not show a clear trend in the early period but a pronounced decrease after 2003, which is similar to the NO_y observation at JFJ. It should be noted that

standard NO_x monitors equipped with Molybdenum converters are cross-sensitive to other NO_y species such as PAN and HNO_3 (Steinbacher et al., 2007). Therefore, these converters overestimate the NO_x concentrations due to the interferences of photochemical species, especially during spring-summer season when sampling photo-chemically aged air masses. The NO_x measurements at remote locations (elevated sites) are thus partially representative of total NO_y species and therefore susceptible to processes at larger scales due to the longer lifetime of NO_y as compared to NO_x .

3.2 Variability in seasonal mean concentrations (1998–2009)

The evolution of seasonal mean NO_y values from 1998–2009 is presented in Fig. 7.

Spring (MAM) and summer (JJA) are displayed in the upper row and autumn (SON) and winter (DJF) in the lower row. The plot shows 3-monthly mean and median values and the range between the lower 25 % and upper 75 % quantiles for each season. Highest NO_y mean and median values were found in 2003 due to the heat wave. Warmer temperatures and intense solar radiation during the heat wave favor NO_x oxidation to HNO_3 and other species. Important factors contributing to this maximum were likely reduced wet and dry deposition, the stagnation of air masses over Europe, and increased thermally forced vertical transport to Jungfraujoch.

NO_y concentrations at JFJ are largest in spring and summer opposite to what is commonly observed in the PBL. This is most likely due to enhanced convective up-

ward transport enforced by the alpine topography during the warm season, whereas in autumn and winter JFJ is more isolated and air masses are mostly representing undisturbed free tropospheric air (Baltensperger et al., 1997; Nyeki et al., 1998; Zellweger et al., 2003). However, also in the cold season JFJ is frequently influenced by European emissions as evidenced by episodic pollution plumes reaching JFJ. The occurrence of

such plumes explains the differences between mean and median concentrations since median values are much less influenced by rare but strong events and more representative of background values. Interestingly, mean and median concentrations are close to each other in summer indicating that pollution plumes are much less frequent

Long-term in situ measurements of NO_x and NO_y at Jungfraujoch

S. Pandey Deolal et al.

[Title Page](#)

[Abstract](#)

[Introduction](#)

[Conclusions](#)

[References](#)

[Tables](#)

[Figures](#)

◀

▶

[Back](#)

[Close](#)

[Full Screen / Esc](#)

[Printer-friendly Version](#)

[Interactive Discussion](#)



or vigorous despite the generally high NO_y concentrations in summer. We interpret this as being the result of more frequent and stronger vertical mixing in summer which creates a better mixed vertical profile and therefore smaller contrasts between periods of upward transport from the PBL and periods dominated by free tropospheric air.

5 The larger influence of regional (European) sources in summer versus more remote sources in winter offers the opportunity to study long-term changes separately for different source regions. Due to the emission reduction measures in Europe a negative trend in NO_y would be expected in spring and summer when JFJ is most strongly influenced by air from the European PBL. However, the trends are superimposed by a
10 large inter annual variability in NO_y which suggests that the extent of exposure to free tropospheric versus European PBL air varies considerably between years. A decline from 1998–2009 (except for 2003) is only observed in the median values for the autumn (SON) season while a decrease in summer is only found for the recent years after 2003. According to some studies, intercontinental transport from North America
15 and Asia has the largest influence on European air in spring and autumn (Wild and Akimoto, 2001; Fiore et al., 2009). The decrease in autumn might therefore be related to the significant reduction in anthropogenic NO_x emissions over North America from 1999–2005 due to the implementation of pollution control technologies in the energy production sector especially in the eastern United States (Kim et al., 2006). However,
20 winter measurements do not confirm this tendency but rather show a large inter-annual variability.

The NO_x measurements also display a large variability in mean and median values in all seasons except summer (Fig. 8). In contrast to NO_y , the NO_x concentrations show a minimum in summer with little variability compared to other seasons. Due to enhanced photochemistry NO_x is rapidly converted to oxidized species like PAN, HNO_3 and particulate nitrates in summer which explains the low NO_x/NO_y ratio in summer (see Fig. 9). However, in other months NO_x mean values are much higher than median values suggesting a large influence of short pollution episodes. Mean values are therefore mostly above the 75 % percentiles of the data. This indicates that except for
25

Long-term in situ measurements of NO_x and NO_y at Jungfraujoch

S. Pandey Deolal et al.

[Title Page](#)

[Abstract](#)

[Introduction](#)

[Conclusions](#)

[References](#)

[Tables](#)

[Figures](#)

◀

▶

[Back](#)

[Close](#)

[Full Screen / Esc](#)

[Printer-friendly Version](#)

[Interactive Discussion](#)



summer the lifetime of NO_x is long enough that rapid upward transport to JFJ can generate large NO_x pollution events. The NO_x measurements do not exhibit any general tendency which is quite unexpected as NO_x emissions decreased in Europe. Similar to the NO_y decrease in the autumn season, NO_x median values also show a slightly decreasing tendency in the autumn months. NO_x is a major contributor to NO_y in autumn and winter but shows a large year to year variability even in the median values, so that it is difficult to detect any trends. A significant decreasing trend in NO_2 concentrations at JFJ from 1995–2007 was reported by Gilge et al. (2010). This is true when considering the earliest measurements of NO_x since a linear trend is mainly determined by the high concentrations of NO_x in 1995–1997 which were influenced by local construction activity (Forrer et al., 2000).

Long term changes in NO_x/NO_y ratios calculated from the hourly concentrations are presented in Fig. 9. The ratio NO_x/NO_y reflects the degree of conversion of NO_x into its oxidation products. The ratio decreases with increasing age of the air parcel, as the lifetime of NO_x is shorter compared to NO_y (Bertman et al., 1995; Singh et al., 2007; Martin et al., 2008). The summer season (JJA) shows the lowest ratios due to the strong photochemical activity and correspondingly low lifetime of NO_x . In autumn and winter the ratios are mostly in the range 0.3–0.6, somewhat lower in spring, and only around 0.2 in summer. The large variability during the autumn and winter months again reflects the strong influence of episodic pollution events. Overall, the NO_x/NO_y series do not exhibit any trend, but remained relatively constant indicating that there has been no strong long-term change in photochemical processing of air masses reaching JFJ.

The contribution of PAN to NO_y is quite important as it can be transported over long distances leading to intercontinental transport of reactive nitrogen species (Bottenheim et al., 1986; Singh, 1987; Singh et al., 1992a). However, PAN is not regularly measured at JFJ and so far two extensive continuous PAN measurements were performed in 1997–1998 by Zellweger et al. (2000) and in 2008, 2009–2010 by Pandey Deolal et al. (2011) and two campaign measurements during February/March 2003 by Whalley et al. (2004) and February 2005–August 2006 by Balzani Loov et al. (2008). PAN/ NO_y

Long-term in situ measurements of NO_x and NO_y at Jungfraujoch

S. Pandey Deolal et al.

[Title Page](#)

[Abstract](#)

[Introduction](#)

[Conclusions](#)

[References](#)

[Tables](#)

[Figures](#)

◀

▶

◀

▶

[Back](#)

[Close](#)

[Full Screen / Esc](#)

[Printer-friendly Version](#)

[Interactive Discussion](#)



ratios from 1997–1998 were compared to 2009–2010 and did not show any significant changes. Both these periods agreed quite well and showed that the average PAN contribution to NO_y was 40 % in 1997–1998 and 37 % in 2009–2010 during the spring and summer whereas NO_x is the dominant contributor in the autumn-winter season contributing up to 51 % (Pandey Deolal et al., 2011).

3.3 Instrument evaluation campaign in 2009–2010

A measurement campaign was conducted in 2009–2010 to evaluate Empa's NO_y and NO measurements using a second NO/ NO_y instrument with high sensitivity and different converter set up deployed at Jungfraujoch by ETHZ (see Sect. 2.2 for instrument details). The measurements started in October 2009 and lasted for 4 months i.e. October, December, January and February. Ten-minute averages of NO_y and NO from both measurement systems are shown in Figs. 10 and 11, respectively. The NO_y and NO data series from 24–31 October were excluded due to contamination from construction activity in the Jungfraujoch railway tunnel. In December the ETHZ instrument had a technical problem causing a gap from 23–31 December.

The ten-minute averages of NO_y were generally in good agreement in October and December. Scatter plots between the ETHZ and Empa measurements in the two months confirm this good correspondence (Fig. 12). However, in October (purple crosses) a number of data points were well below the 1:1 line indicating episodic NO_y peaks observed by the ETHZ but not the Empa instrument (Fig. 12). A possible reason for such peaks is touristic activity during the daytime as ETHZ sampling inlet was more close to touristic terrace. To test this hypothesis we filtered the dataset for nighttime observations (black circles) only. In the plot, the December data (green crosses) show many data points above the 1:1 line indicating higher NO_y concentrations in Empa's measurements which is likely explained by the rapid drop in converter efficiency in ETHZ gold converter (see Fig. 3) after the first ten days of December. Under such conditions species like HNO_3 may have even lower conversion efficiency than NO_2 for which the efficiency was determined, resulting in an underestimation of NO_y .

Long-term in situ measurements of NO_x and NO_y at Jungfraujoch

S. Pandey Deolal et al.

[Title Page](#)

[Abstract](#)

[Introduction](#)

[Conclusions](#)

[References](#)

[Tables](#)

[Figures](#)

◀

▶

◀

▶

[Back](#)

[Close](#)

[Full Screen / Esc](#)

[Printer-friendly Version](#)

[Interactive Discussion](#)



Long-term in situ measurements of NO_x and NO_y at Jungfraujoch

S. Pandey Deolal et al.

[Title Page](#)[Abstract](#)[Introduction](#)[Conclusions](#)[References](#)[Tables](#)[Figures](#)[◀](#)[▶](#)[Back](#)[Close](#)[Full Screen / Esc](#)[Printer-friendly Version](#)[Interactive Discussion](#)

concentrations. Therefore, only the first ten days of nighttime measurements in December were included in the calculation of a linear regression. An orthogonal linear fit to all October and 1–10 December nighttime (12:00 a.m.–06:00 a.m. UTC) data accounting for errors from both instruments yielded a slope of 0.89 ± 0.004 and an intercept of $(19 \pm 3 \text{ ppt})$ with a correlation coefficient of $R^2 = 0.97$ for $N = 1765$ observations.

In summary, the result for the filtered data (black circles in Fig. 12) is

$$\text{NO}_y\text{-Empa} = (0.89 \pm 0.004) \cdot \text{NO}_y\text{-ETHZ} + (19 \pm 3) \text{ ppt}, R^2 = 0.97 \quad (2)$$

The results presented in Fig. 12 indicate that the Empa measurements are on the order of 10 % lower than those by ETHZ when excluding all problematic measurements.

The lower NO_y values could potentially be due to wall losses of HNO₃ in the long sampling inlet. However, the comparison between the NO measurements from the two instruments (not shown), which are not affected by such losses, reveals differences of the same order of magnitude in the daytime and therefore no firm conclusion can be drawn on the source of the differences between the two NO_y measurements.

3.4 Possible influences of snow photochemistry and local contamination

Snow photochemistry: unlike the previous two months, the NO_y measurements in January and February did not agree except for a few short periods as shown in Fig. 10. The NO_y inlet of ETHZ turned out not to protect sufficiently against heavy snow fall and as a consequence the measurements in January and February suffered from snow covering the tip of the NO and NO_y inlets. Although these measurements cannot be trusted in absolute terms, they provide some interesting insights into the problem of NO_y photochemistry on snow surfaces which may affect any observations over snow-covered surfaces.

In January and February, the NO_y measurements of ETHZ showed a systematic diurnal cycle with an afternoon maximum not observed in the Empa measurements (Fig. 10). At the time of the maximum the ETHZ NO_y concentrations were >3 times higher than those measured by Empa, particularly in January. To further evaluate

Long-term in situ measurements of NO_x and NO_y at Jungfraujoch

S. Pandey Deolal et al.

[Title Page](#)

[Abstract](#)

[Introduction](#)

[Conclusions](#)

[References](#)

[Tables](#)

[Figures](#)

[◀](#)

[▶](#)

[◀](#)

[▶](#)

[Back](#)

[Close](#)

[Full Screen / Esc](#)

[Printer-friendly Version](#)

[Interactive Discussion](#)



these measurements they were compared with sunshine data and wind speed data taken from meteorological and climatological data base (CLIMAP-net, MeteoSwiss). The problem of contamination was more severe in January and therefore the influence of snow photochemistry is demonstrated for this month. Time series of NO_y concentrations and sunshine are shown in Fig. 13. Days with fresh snowfall are denoted with a star symbol. The periodic diurnal peaks of ETHZ data were clearly correlated with sunshine days. The correlation with wind speed presented in Fig. 14 additionally suggests that the pronounced diurnal cycles in the ETHZ NO_y measurements were mostly observed on days with low wind speed. NO exhibits a pronounced diurnal cycle in both measurements but the maximum around noon was almost a factor 3 higher for ETHZ than for Empa (not shown). The elevated NO_y and NO concentrations in the ETHZ measurements, which are clearly correlated with sunshine, thus strongly point towards photochemical production of nitrogen oxides in the snow covered inlet.

Several previous studies indicated that nitrogen containing species adsorbed and dissolved in snow in the form of NO₃⁻ may be photolyzed to release NO_x from the snow pack and potentially contribute to NO_x emission in the boundary layer (Honrath et al., 1999; Domine and Shepson, 2002; Grannas et al., 2007). At Summit, Greenland, for example, NO_x levels in the interstitial air were 3 to >10 times higher than those in ambient air and greater than ambient NO_y levels (Honrath et al., 1999).

Grannas et al. (2007) suggested that nitrate photolysis in the aqueous phase proceeds by the following two channels.



Where Reaction (R1) exceeds Reaction (R2) by a factor 8 to 9. Therefore, we hypothesize that the periodic peaks found in the ETHZ NO_y data were primarily due to NO₂ emissions from fresh snow. Subsequent partial photolysis of the NO₂ released from the snow would also explain the increase in NO which was on average 3–4 times lower than the increase in NO_y.

Although the situation with a snow-covered inlet represents an extreme case and no quantitative information can be derived from this inadvertent experiment, the results are raising the question to what extent snow photochemistry might impact the measurements at a high alpine site such as Jungfraujoch which is snow-covered all year-round. However, the Empa system did not show such an increase in NO_y during daytime in January, suggesting that snow photochemistry did not significantly impact the measurements, at least during this month. However, it would be desirable to perform additional more quantitative experiments in the future to assess the potential role of snow photochemistry for the NO_x and NO_y measurements at JFJ in detail.

Local influence: as mentioned earlier and also pointed out in other studies the measurements are occasionally influenced by local contamination sources such as diesel emissions from a snowcat used for tourist purposes in the warm season affecting the aerosol concentrations (Collaud Coen et al., 2011), construction activity (Forrer et al., 2000), and other activities including cigarette smoking on touristic terrace. Therefore, we analyzed the daytime and nighttime trends of NO_y and NO_x separately since, except for construction activity, such influences are expected to be minimal at nighttime. Figure 15 presents the time series of monthly median NO_y concentrations separately for nighttime (00:00 h–06:00 h local time) and daytime (08:00 h–18:00 h local time). The Fig. 15 reveals that no significant differences exist between trends in the nighttime and daytime measurements, a finding which also holds for NO_x . This suggests that despite episodic influences local contamination has no significant impact on the long term measurements. It should be noted, that contamination events, particularly those related to construction activities, are always filtered up to the best possible information and not included in the measurement data series.

25 4 Conclusions

Changes in NO_y concentrations at the high alpine site Jungfraujoch, which are expected to be representative for the lower free troposphere over Europe, were

[Title Page](#)[Abstract](#)[Introduction](#)[Conclusions](#)[References](#)[Tables](#)[Figures](#)[◀](#)[▶](#)[◀](#)[▶](#)[Back](#)[Close](#)[Full Screen / Esc](#)[Printer-friendly Version](#)[Interactive Discussion](#)

Long-term in situ measurements of NO_x and NO_y at Jungfraujoch

S. Pandey Deolal et al.

[Title Page](#)

[Abstract](#)

[Introduction](#)

[Conclusions](#)

[References](#)

[Tables](#)

[Figures](#)

[◀](#)

[▶](#)

[◀](#)

[▶](#)

[Back](#)

[Close](#)

[Full Screen / Esc](#)

[Printer-friendly Version](#)

[Interactive Discussion](#)



investigated for the period 1998–2009. Considering the whole period, the time series does not show a clear trend but rather a maximum in the years 2002 to 2004 and a decline thereafter. The largest annual average of NO_y was measured in 2003 with a large positive anomaly coinciding with a maximum in O_3 . These high values were related to the European heat wave and were probably caused by a combination of effects including stagnation of air masses over Europe and reduced wet deposition of NO_y . If analyzed by season, the long-term changes in NO_y reveal some differences: autumn (SON) values show a decrease in median values (except for the year 2003) which might be due to decreasing NO_x emissions over Europe and North America. Other seasons, however, do not reveal a clear trend. NO_x measurements at Jungfraujoch do not show any significant changes but rather a large interannual variability. Except for summer, the seasonal mean NO_x concentrations are strongly controlled by episodic pollution events explaining the large interannual variability which obscures any long-term trend. The median values, which are expected to be less influenced by short pollution plumes, show some decreasing tendency in the autumn season in recent years consistent with the NO_y decrease but otherwise no overall trend is observed. This is different from NO_x measurements at low elevation in Switzerland which show a clear decreasing trend at both urban and rural sites over the investigation period. NO_x changes at medium elevation sites in Switzerland (at 1000 to 1600 m a.m.s.l.) exhibit some similarity with NO_y changes at Jungfraujoch, i.e. large variability in the early years and a decrease in recent years. The high interannual variability in the early years is likely related to several biomass burning episodes (Yurganov et al., 2005b) and the El-Nino event in 1998 (Koumoutsaris et al., 2008), as it is also observed in the CO measurements.

The comparison between the ETHZ and Empa NO_y measurements showed on average 10 % lower values in Empa's instrument including all uncertainties and errors. This may point to minor losses of HNO_3 in the Empa's sampling inlet, which is in agreement with the earlier inter-comparison performed in spring 1998 by Carpenter et al. (2000). However, significant deviations were observed between ETHZ and Empa measurements particularly during day time with higher concentrations measured by

ETHZ instrument indicating some influences from the immediate vicinity (touristic platform). However, local contaminations from touristic activity or other sources do not impart the long term changes as demonstrated by a comparison of daytime and night-time measurements.

5 A large discrepancy between the two measurements was observed in January and February when ETHZ measurements exhibited a pronounced diurnal cycle. The likely explanation for this behavior was snow accumulation in the inlet, which caused >3 times higher NO_y concentrations measured by the ETHZ instrument favored by photochemistry and low wind speed. It is quite challenging to assess whether the long-term

10 NO_y measurements can be influenced by snow photochemistry since the Jungfraujoch observatory is situated between snow covered mountains. Therefore an additional study would be helpful to address this issue in more detail.

Acknowledgements. We thank the Swiss National Foundation (SNF) for funding this project and support of the international foundation for high-alpine research stations Jungfraujoch and

15 Gornergrat (HFSJG) is highly appreciated.

References

BAFU: NABEL – Luftbelastung 2009. Messresultate des Nationalen Beobachtungsnetzes für Luftfremdstoffe (NABEL). Umwelt-Zustand Nr. 1016. Bundesamt für Umwelt, Bern, 142 pp., available at: <http://www.umwelt-schweiz.ch/uz-1016-d>, 2010 (in German).

20 Baltensperger, U., Gaggeler, H. W., Jost, D. T., Lugauer, M., Schwikowski, M., Weingartner, E., and Seibert, P.: Aerosol climatology at the high-alpine site Jungfraujoch, Switzerland, *J. Geophys. Res.-Atmos.*, 102, 19707–19715, 1997.

Bertman, S. B., Roberts, J. M., Parrish, D. D., Buhr, M. P., Goldan, P. D., Kuster, W. C., Fehsenfeld, F. C., Montzka, S. A., and Westberg, H.: Evolution of alkyl nitrates with air mass age, *J. Geophys. Res.-Atmos.*, 100, 22805–22813, 1995.

25 Bollinger, M. J., Sievers, R. E., Fahey, D. W., and Fehsenfeld, F. C.: Conversion of Nitrogen Dioxide, Nitric-Acid, and normal-Propyl Nitrate to Nitric Oxide by Gold-Catalyzed Reduction with Carbon-Monoxide, *Anal. Chem.*, 55, 1980–1986, 1983.

[Title Page](#)

[Abstract](#)

[Introduction](#)

[Conclusions](#)

[References](#)

[Tables](#)

[Figures](#)

◀

▶

[Back](#)

[Close](#)

[Full Screen / Esc](#)

[Printer-friendly Version](#)

[Interactive Discussion](#)



Bottenheim, J. W., Gallant, A. G., and Brice, K. A.: Measurements of NO_y Species and O-3 at 82-Degrees-N Latitude, *Geophys. Res. Lett.*, 13, 113–116, 1986.

Bronnimann, S., Schuepbach, E., Zanis, P., Buchmann, B., and Wanner, H.: A climatology of regional background ozone at different elevations in Switzerland (1992–1998), *Atmos. Environ.*, 34, 5191–5198, 2000.

Brunner, D., Staehelin, J., and Jeker, D.: Large-scale nitrogen oxide plumes in the tropopause region and implications for ozone, *Science*, 282, 1305–1309, 1998.

Carpenter, L. J., Green, T. J., Mills, G. P., Bauguitte, S., Penkett, S. A., Zanis, P., Schuepbach, E., Schmidbauer, N., Monks, P. S., and Zellweger, C.: Oxidized nitrogen and ozone production efficiencies in the springtime free troposphere over the Alps, *J. Geophys. Res.-Atmos.*, 105, 14547–14559, 2000.

Collaud Coen, M., Weingartner, E., Furger, M., Nyeki, S., Prévôt, A. S. H., Steinbacher, M., and Baltensperger, U.: Aerosol climatology and planetary boundary influence at the Jungfraujoch analyzed by synoptic weather types, *Atmos. Chem. Phys.*, 11, 5931–5944, doi:10.5194/acp-11-5931-2011, 2011.

Cui, J., Deolal Pandey, S., Sprenger, M., Henne, S., Staehelin, J., Steinbacher, M., and Nédélec, P.: Free tropospheric ozone changes over Europe as observed at Jungfraujoch (1990–2008): An analysis based on backward trajectories, *J. Geophys. Res.*, 116, D10304, doi:10.1029/2010JD015154, 2011.

Day, D. A., Dillon, M. B., Wooldridge, P. J., Thornton, J. A., Rosen, R. S., Wood, E. C., and Cohen, R. C.: On alkyl nitrates, O_3 , and the “missing NOy”, *J. Geophys. Res.-Atmos.*, 108, ACH 7-1, doi:10.1029/2003JD003685, 2003.

Derwent, R. G., Jenkin, M. E., Saunders, S. M., Pilling, M. J., Simmonds, P. G., Passant, N. R., Dollard, G. J., Dumitrescu, P., and Kent, A.: Photochemical ozone formation in north west Europe and its control, *Atmos. Environ.*, 37, 1983–1991, doi:10.1016/S1352-2310(03)00031-1, 2003.

Domine, F. and Shepson, P. B.: Air-snow interactions and atmospheric chemistry, *Science*, 297, 1506–1510, 2002.

Drummond, J. W., Volz, A., and Ehhalt, D. H.: An Optimized Chemiluminescence Detector for Tropospheric NO Measurements, *J. Atmos. Chem.*, 2, 287–306, 1985.

Emmons, L. K., Carroll, M. A., Hauglustaine, D. A., Brasseur, G. P., Atherton, C., Penner, J., Sillman, S., Levy, H., Rohrer, F., Wauben, W. M. F., VanVelthoven, P. F. J., Wang, Y., Jacob, D., Bakwin, P., Dickerson, R., Doddridge, B., Gerbig, C., Honrath, R., Hubler, G., Jaffe, D.,

Long-term in situ measurements of NO_x and NO_y at Jungfraujoch

[Title Page](#)

[Abstract](#)

[Introduction](#)

[Conclusions](#)

[References](#)

[Tables](#)

[Figures](#)

◀

▶

◀

▶

[Back](#)

[Close](#)

[Full Screen / Esc](#)

[Printer-friendly Version](#)

[Interactive Discussion](#)



Long-term in situ measurements of NO_x and NO_y at Jungfraujoch

S. Pandey Deolal et al.

[Title Page](#)

[Abstract](#)

[Introduction](#)

[Conclusions](#)

[References](#)

[Tables](#)

[Figures](#)

◀

▶

◀

▶

[Back](#)

[Close](#)

[Full Screen / Esc](#)

[Printer-friendly Version](#)

[Interactive Discussion](#)



Long-term in situ measurements of NO_x and NO_y at Jungfraujoch

S. Pandey Deolal et al.

[Title Page](#)

[Abstract](#)

[Introduction](#)

[Conclusions](#)

[References](#)

[Tables](#)

[Figures](#)

◀

▶

◀

▶

[Back](#)

[Close](#)

[Full Screen / Esc](#)

[Printer-friendly Version](#)

[Interactive Discussion](#)



Hutterli, M., Jacobi, H. W., Klán, P., Lefer, B., McConnell, J., Plane, J., Sander, R., Savarino, J., Shepson, P. B., Simpson, W. R., Sodeau, J. R., von Glasow, R., Weller, R., Wolff, E. W., and Zhu, T.: An overview of snow photochemistry: evidence, mechanisms and impacts, *Atmos. Chem. Phys.*, 7, 4329–4373, doi:10.5194/acp-7-4329-2007, 2007.

5 Harrison, R. M., Grenfell, J. L., Yamulki, S., Clemitschaw, K. C., Penkett, S. A., Cape, J. N., and McFadyen, G. G.: Budget of NO_y species measured at a coastal site, *Atmos. Environ.*, 33, 4255–4272, 1999.

10 Hayden, K. L., Anlauf, K. G., Hastie, D. R., and Bottenheim, J. W.: Partitioning of reactive atmospheric nitrogen oxides at an elevated site in southern Quebec, Canada, *J. Geophys. Res.-Atmos.*, 108, ACH 2-1, doi:10.1029/2002JD003188, 2003.

15 Hegglin, M. I., Brunner, D., Peter, T., Hoor, P., Fischer, H., Staehelin, J., Krebsbach, M., Schiller, C., Parchatka, U., and Weers, U.: Measurements of NO, NO_y, N₂O, and O₃ during SPURT: implications for transport and chemistry in the lowermost stratosphere, *Atmos. Chem. Phys.*, 6, 1331–1350, doi:10.5194/acp-6-1331-2006, 2006.

20 Honrath, R. E., Peterson, M. C., Guo, S., Dibb, J. E., Shepson, P. B., and Campbell, B.: Evidence of NO_x production within or upon ice particles in the Greenland snowpack, *Geophys. Res. Lett.*, 26, 695–698, 1999.

25 Kaiser, A., Schelfinger, H., Spangl, W., Weiss, A., Gilge, S., Fricke, W., Ries, L., Cemas, D., and Jesenovec, B.: Transport of nitrogen oxides, carbon monoxide and ozone to the Alpine Global Atmosphere Watch stations Jungfraujoch (Switzerland), Zugspitze and Hohenpeissenberg (Germany), Sonnblick (Austria) and Mt. Krvavec (Slovenia), *Atmos. Environ.*, 41, 9273–9287, doi:10.1016/j.atmosenv.2007.09.027, 2007.

30 Kim, S. W., Heckel, A., McKeen, S. A., Frost, G. J., Hsie, E. Y., Trainer, M. K., Richter, A., Burrows, J. P., Peckham, S. E., and Grell, G. A.: Satellite-observed US power plant NO_x emission reductions and their impact on air quality, *Geophys. Res. Lett.*, 33, 1–5, doi:10.1029/2006GL027749, 2006.

Koumoutsaris, S., Bey, I., Generoso, S., and Thouret, V.: Influence of El Nino-Southern Oscillation on the interannual variability of tropospheric ozone in the northern midlatitudes, *J. Geophys. Res.-Atmos.*, 113, 1–21, doi:10.1029/2007JD009753, 2008.

35 Lange, L., Fischer, H., Parchatka, U., Gurk, C., Zenker, T., and Harris, G. W.: Characterization and application of an externally mounted catalytic converter for aircraft measurements of NO_y, *Rev. Sci. Instrum.*, 73, 3051–3057, doi:10.1063/1.1488680, 2002.

Levy, H.: Normal Atmosphere: Large Radical and Formaldehyde Concentrations Predicted,

Levy, H., Moxim, W. J., Klonecki, A. A., and Kasibhatla, P. S.: Simulated tropospheric NO_x : Its evaluation, global distribution and individual source contributions, *J. Geophys. Res.-Atmos.*, 104, 26279–26306, 1999.

5 Logan, J. A., Prather, M. J., Wofsy, S. C., and McElroy, M. B.: Tropospheric Chemistry: A Global Perspective, *J. Geophys. Res.*, 86(C8), 7210–7254, doi:10.1029/JC086iC08p07210, 1981.

Logan, J. A.: Nitrogen Oxides in the Troposphere – Global and Regional Budgets, *J. Geophys. Res.-Oc. Atm.*, 88, 785–807, 1983.

10 Loov, J. M. B., Henne, S., Legreid, G., Staehelin, J., Reimann, S., Prevot, A. S. H., Steinbacher, M., and Vollmer, M. K.: Estimation of background concentrations of trace gases at the Swiss Alpine site Jungfraujoch (3580 m asl), *J. Geophys. Res.-Atmos.*, 113, 1–17, doi:10.1029/2007JD009751, 2008.

15 Lugauer, M., Baltensperger, U., Furger, M., Gaggeler, H. W., Jost, D. T., Schwikowski, M., and Wanner, H.: Aerosol transport to the high Alpine sites Jungfraujoch (3454 m asl) and Colle Gnifetti (4452 m asl), *Tellus B*, 50, 76–92, 1998.

Luterbacher, J., Dietrich, D., Xoplaki, E., Grosjean, M., and Wanner, H.: European seasonal and annual temperature variability, trends, and extremes since 1500, *Science*, 303, 1499–1503, 2004.

20 Martin, M. V., Honrath, R. E., Owen, R. C., and Li, Q. B.: Seasonal variation of nitrogen oxides in the central North Atlantic lower free troposphere, *J. Geophys. Res.-Atmos.*, 113, 1–15, doi:10.1029/2007JD009688, 2008.

25 Nyeki, S., Baltensperger, U., Colbeck, I., Jost, D. T., Weingartner, E., and Gaggeler, H. W.: The Jungfraujoch high-Alpine research station (3454 m) as a background clean continental site for the measurement of aerosol parameters, *J. Geophys. Res.-Atmos.*, 103, 6097–6107, 1998.

Ordóñez, C., Brunner, D., Staehelin, J., Hadjinicolaou, P., Pyle, J. A., Jonas, M., Wernli, H., and Prevot, A. S. H.: Strong influence of lowermost stratospheric ozone on lower tropospheric background ozone changes over Europe, *Geophys. Res. Lett.*, 34, L07805, doi:10.1029/2006GL029113, 2007.

30 Pandey Deolal, S., Cui, J., Brunner, D., Henne, S., Weers, U., Steinbacher, M., and Staehelin, J.: Long range transport of PAN and NO_y at Jungfraujoch, in preparation, 2011.

Pätz, H.-W., Volz-Thomas, A., Hegglin, M. I., Brunner, D., Fischer, H., and Schmidt, U.: In-situ comparison of the NO_y instruments flown in MOZAIC and SPURT, *Atmos. Chem. Phys.*, 6,

Long-term in situ measurements of NO_x and NO_y at Jungfraujoch

S. Pandey Deolal et al.

[Title Page](#)

[Abstract](#)

[Introduction](#)

[Conclusions](#)

[References](#)

[Tables](#)

[Figures](#)

◀

▶

◀

▶

[Back](#)

[Close](#)

[Full Screen / Esc](#)

[Printer-friendly Version](#)

[Interactive Discussion](#)



Schär, C., Vidale, P. L., Luthi, D., Frei, C., Haberli, C., Liniger, M. A., and Appenzeller, C.: The role of increasing temperature variability in European summer heatwaves, *Nature*, 427, 332–336, doi:10.1038/nature02300, 2004.

5 Schaub, D., Brunner, D., Boersma, K. F., Keller, J., Folini, D., Buchmann, B., Berresheim, H., and Staehelin, J.: SCIAMACHY tropospheric NO₂ over Switzerland: estimates of NO_x lifetimes and impact of the complex Alpine topography on the retrieval, *Atmos. Chem. Phys.*, 7, 5971–5987, doi:10.5194/acp-7-5971-2007, 2007.

10 Simmonds, P. G., Manning, A. J., Derwent, R. G., Ciais, P., Ramonet, M., Kazan, V., and Ryall, D.: A burning question. Can recent growth rate anomalies in the greenhouse gases be attributed to large-scale biomass burning events?, *Atmos. Environ.*, 39, 2513–2517, doi:10.1016/j.atmosenv.2005.02.018, 2005.

Singh, H. B.: Reactive Nitrogen in the Troposphere, *Environ. Sci. Technol.*, 21, 320–327, 1987.

Singh, H. B., Herlth, D., Ohara, D., Zahnle, K., Bradshaw, J. D., Sandholm, S. T., Talbot, R., 15 Crutzen, P. J., and Kanakidou, M.: Relationship of Peroxyacetyl Nitrate to Active and Total Odd Nitrogen at Northern High-Latitudes: Influence of Reservoir Species on NO_x and O₃, *J. Geophys. Res.-Atmos.*, 97, 16523–16530, 1992a.

Singh, H. B., Ohara, D., Herlth, D., Bradshaw, J. D., Sandholm, S. T., Gregory, G. L., Sachse, G. W., Blake, D. R., Crutzen, P. J., and Kanakidou, M. A.: Atmospheric Measurements of Peroxyacetyl Nitrate and Other Organic Nitrates at High Latitudes: Possible Sources and Sinks, *J. Geophys. Res.-Atmos.*, 97, 16511–16522, 1992b.

Singh, H. B., Salas, L., Herlth, D., Kolyer, R., Czech, E., Avery, M., Crawford, J. H., Pierce, R. B., Sachse, G. W., Blake, D. R., Cohen, R. C., Bertram, T. H., Perring, A., Wooldridge, P. J., Dibb, J., Huey, G., Hudman, R. C., Turquety, S., Emmons, L. K., Flocke, F., Tang, Y., Carmichael, G. R., and Horowitz, L. W.: Reactive nitrogen distribution and partitioning in the North American troposphere and lowermost stratosphere, *J. Geophys. Res.-Atmos.*, 112, 1–15, doi:10.1029/2006JD007664, 2007.

Steinbacher, M., Zellweger, C., Schwarzenbach, B., Bugmann, S., Buchmann, B., Ordonez, C., Prevot, A. S. H., and Hueglin, C.: Nitrogen oxide measurements at rural sites in Switzerland: Bias of conventional measurement techniques, *J. Geophys. Res.-Atmos.*, 112, D11307, doi:10.1029/2006JD007971, 2007.

30 Stohl, A., Trainer, M., Ryerson, T. B., Holloway, J. S., and Parrish, D. D.: Export of NO_y from the North American boundary layer during 1996 and 1997 North Atlantic Regional Experiments,

Long-term in situ measurements of NO_x and NO_y at Jungfraujoch

S. Pandey Deolal et al.

[Title Page](#)

[Abstract](#)

[Introduction](#)

[Conclusions](#)

[References](#)

[Tables](#)

[Figures](#)

◀

▶

◀

▶

[Back](#)

[Close](#)

[Full Screen / Esc](#)

[Printer-friendly Version](#)

[Interactive Discussion](#)



Thakur, A. N., Singh, H. B., Mariani, P., Chen, Y., Wang, Y., Jacob, D. J., Brasseur, G., Muller, J. F., and Lawrence, M.: Distribution of reactive nitrogen species in the remote free troposphere: data and model comparisons, *Atmos. Environ.*, 33, 1403–1422, 1999.

5 Thornberry, T., Carroll, M. A., Keeler, G. J., Sillman, S., Bertman, S. B., Pippin, M. R., Ostling, K., Grossenbacher, J. W., Shepson, P. B., Cooper, O. R., Moody, J. L., and Stockwell, W. R.: Observations of reactive oxidized nitrogen and speciation of NO_y during the PROPHET summer 1998 intensive, *J. Geophys. Res.-Atmos.*, 106, 24359–24386, 2001.

10 Tressol, M., Ordonez, C., Zbinden, R., Brioude, J., Thouret, V., Mari, C., Nedelev, P., Cammas, J.-P., Smit, H., Patz, H.-W., and Volz-Thomas, A.: Air pollution during the 2003 European heat wave as seen by MOZAIC airliners, *Atmos. Chem. Phys.*, 8, 2133–2150, doi:10.5194/acp-8-2133-2008, 2008.

15 Wennberg, P. O., Hanisco, T. F., Jaegle, L., Jacob, D. J., Hintsa, E. J., Lanzendorf, E. J., Anderson, J. G., Gao, R. S., Keim, E. R., Donnelly, S. G., Del Negro, L. A., Fahey, D. W., McKeen, S. A., Salawitch, R. J., Webster, C. R., May, R. D., Herman, R. L., Proffitt, M. H., Margitan, J. J., Atlas, E. L., Schauffler, S. M., Flocke, F., McElroy, C. T., and Bui, T. P.: Hydrogen radicals, nitrogen radicals, and the production of O₃ in the upper troposphere, *Science*, 279, 49–53, 1998.

20 Whalley, L. K., Lewis, A. C., McQuaid, J. B., Purvis, R. M., Lee, J. D., Stemmler, K., Zellweger, C., and Ridgeon, P.: Two high-speed, portable GC systems designed for the measurement of non-methane hydrocarbons and PAN: Results from the Jungfraujoch High Altitude Observatory, *J. Environ. Monitor.*, 6, 234–241, doi:10.1039/b310022g, 2004.

25 Wild, O. and Akimoto, H.: Intercontinental transport of ozone and its precursors in a three-dimensional global CTM, *J. Geophys. Res.-Atmos.*, 106, 27729–27744, 2001.

Williams, E. J., Roberts, J. M., Baumann, K., Bertman, S. B., Buhr, S., Norton, R. B., and Fehsenfeld, F. C.: Variations in NO_y composition at Idaho Hill, Colorado, *J. Geophys. Res.-Atmos.*, 102, 6297–6314, 1997.

30 Yurganov, L. N., Duchatelet, P., Dzhola, A. V., Edwards, D. P., Hase, F., Kramer, I., Mahieu, E., Mellqvist, J., Notholt, J., Novelli, P. C., Rockmann, A., Scheel, H. E., Schneider, M., Schulz, A., Strandberg, A., Sussmann, R., Tanimoto, H., Velazco, V., Drummond, J. R., and Gille, J. C.: Increased Northern Hemispheric carbon monoxide burden in the troposphere in 2002 and 2003 detected from the ground and from space, *Atmos. Chem. Phys.*, 5, 563–573, doi:10.5194/acp-5-563-2005, 2005.

Long-term in situ measurements of NO_x and NO_y at Jungfraujoch

S. Pandey Deolal et al.

[Title Page](#)

[Abstract](#)

[Introduction](#)

[Conclusions](#)

[References](#)

[Tables](#)

[Figures](#)

◀

▶

◀

▶

[Back](#)

[Close](#)

[Full Screen / Esc](#)

[Printer-friendly Version](#)

[Interactive Discussion](#)



Zanis, P., Schuepbach, E., Scheel, H. E., Baudenbacher, M., and Buchmann, B.: Inhomogeneities and trends in the surface ozone record (1988–1996) at Jungfraujoch in the Swiss Alps, *Atmos. Environ.*, 33, 3777–3786, 1999.

5 Zanis, P., Ganser, A., Zellweger, C., Henne, S., Steinbacher, M., and Staehelin, J.: Seasonal variability of measured ozone production efficiencies in the lower free troposphere of Central Europe, *Atmos. Chem. Phys.*, 7, 223–236, doi:10.5194/acp-7-223-2007, 2007.

Zellweger, C., Ammann, M., Buchmann, B., Hofer, P., Lugauer, M., Ruttimann, R., Streit, N., Weingartner, E., and Baltensperger, U.: Summertime NO_y speciation at the Jungfraujoch, 3580 m above sea level, Switzerland, *J. Geophys. Res.-Atmos.*, 105, 6655–6667, 2000.

10 Zellweger, C., Forrer, J., Hofer, P., Nyeki, S., Schwarzenbach, B., Weingartner, E., Ammann, M., and Baltensperger, U.: Partitioning of reactive nitrogen (NO_y) and dependence on meteorological conditions in the lower free troposphere, *Atmos. Chem. Phys.*, 3, 779–796, doi:10.5194/acp-3-779-2003, 2003.

Zellweger, C., Hüglin, C., Klausen, J., Steinbacher, M., Vollmer, M., and Buchmann, B.: Intercomparison of four different carbon monoxide measurement techniques and evaluation of the long-term carbon monoxide time series of Jungfraujoch, *Atmos. Chem. Phys.*, 9, 3491–3503, doi:10.5194/acp-9-3491-2009, 2009.

Long-term in situ measurements of NO_x and NO_y at Jungfraujoch

S. Pandey Deolal et al.

Title Page

Abstract

Introduction

Conclusions

Figures

1

▶

Back

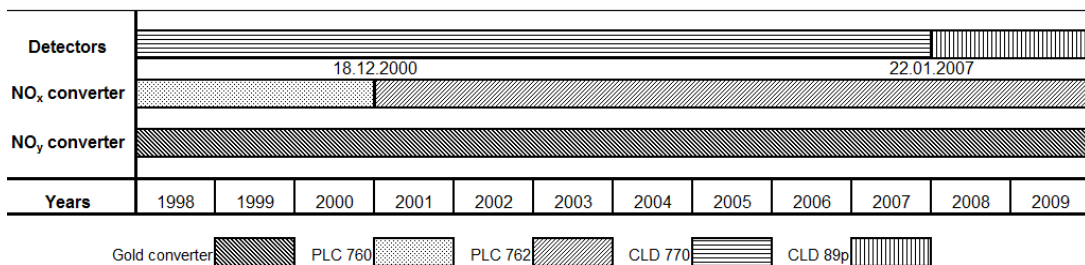
Close

Full Screen / Esc

Interactive Discussion



Table 1. NO_x and NO_y instrumental changes (photolytic converter (PLC), chemiluminescence detectors (CLD) and gold converter) during 1998–2009 at Jungfraujoch.



Long-term in situ measurements of NO_x and NO_y at Jungfraujoch

S. Pandey Deolal et al.

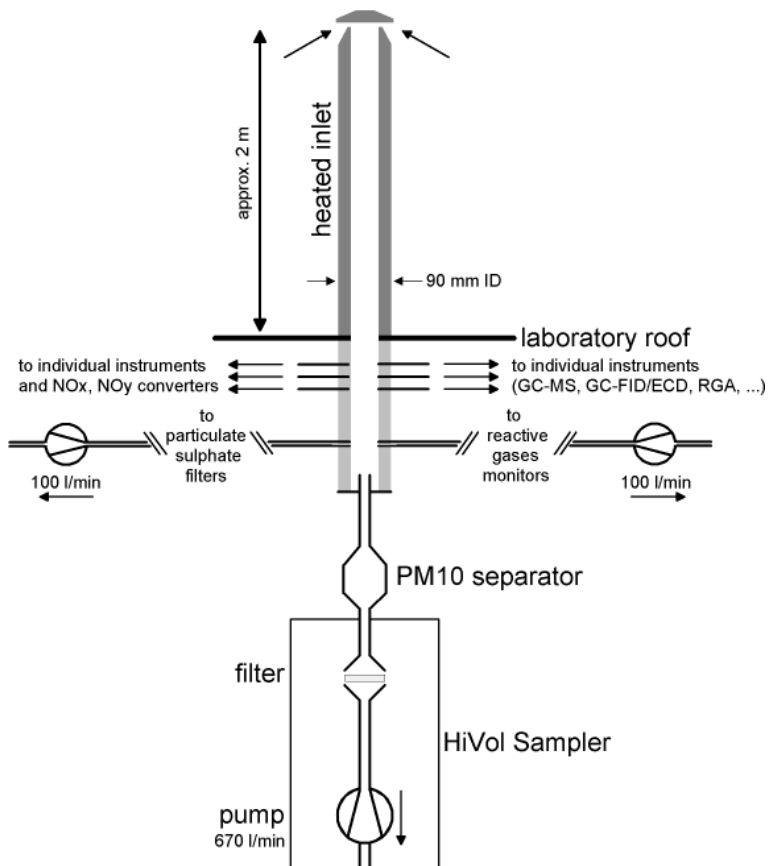


Fig. 1. Schematic of Empa's trace gas inlet at Jungfraujoch.

21861

Long-term in situ measurements of NO_x and NO_y at Jungfraujoch

S. Pandey Deolal et al.

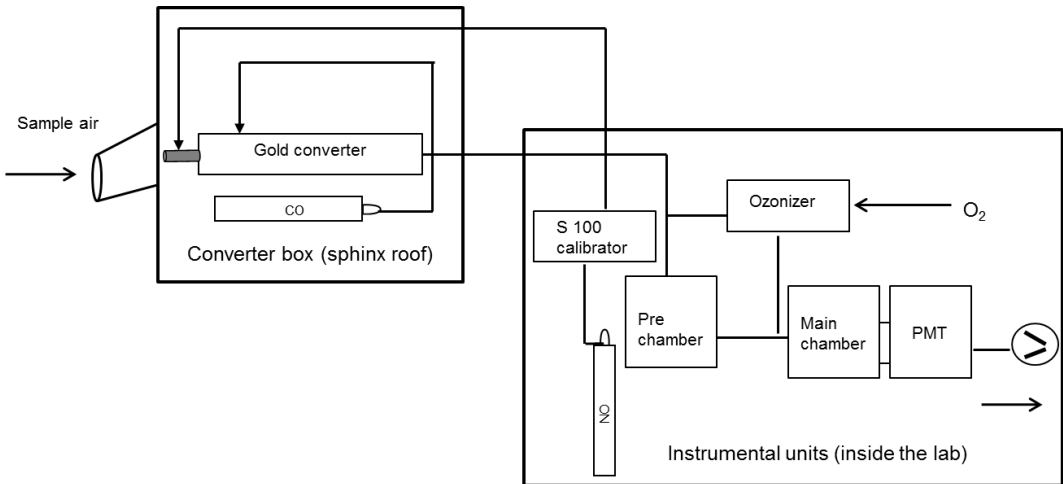


Fig. 2. Schematic of the ETHZ NO_y instrument operated during the campaign (October 2009–February 2010) at Jungfraujoch.

Title Page

Abstract

Introduction

Conclusions

References

Tables

Figures

14

◀

▶

Back

Close

Full Screen / Esc

Printer-friendly Version

Interactive Discussion

Long-term in situ measurements of NO_x and NO_y at Jungfraujoch

S. Pandey Deolal et al.

The scatter plot illustrates the converter efficiency percentage over a period from October 2009 to February 2010. The Y-axis represents 'Converter Efficiency %' with major ticks at 80, 85, 90, 95, and 100. The X-axis represents 'Time' with labels for specific dates: 2-Oct-09, 3-Nov-09, 5-Dec-09, 15-Dec-09, 8-Jan-10, 18-Jan-10, 28-Jan-10, 7-Feb-10, and 17-Feb-10. The data points, shown as black circles, generally trend upwards from late October to early January, followed by a slight dip and then a recovery to near 100% by mid-February. Horizontal dotted grid lines are present at 80, 85, 90, 95, and 100.

Fig. 3. Conversion efficiency of the ETHZ NO_y converter determined by daily GPT (gas phase titrations) calibrations, time (date-month-year).

21863

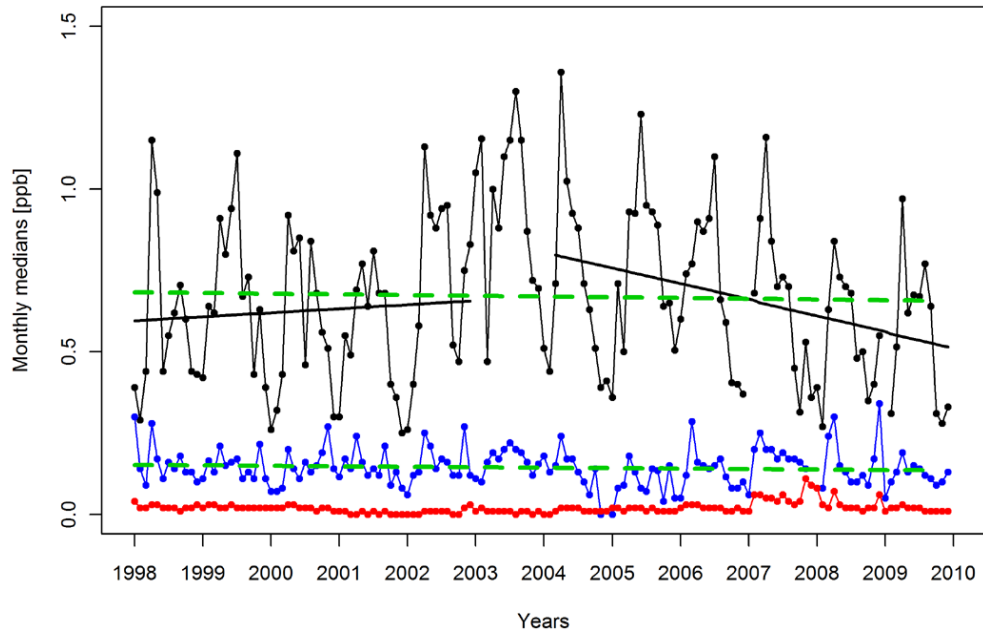


Fig. 4. Monthly median values of NO_y (black), NO_x (blue) and NO (red) from January 1998–December 2009. The black thick lines are linear trends before and after 2003 and green dashed lines represents overall linear trend.

Long-term in situ measurements of NO_x and NO_y at Jungfraujoch

S. Pandey Deolal et al.

[Title Page](#)

[Abstract](#)

[Introduction](#)

[Conclusions](#)

[References](#)

[Tables](#)

[Figures](#)

◀

▶

◀

▶

[Back](#)

[Close](#)

[Full Screen / Esc](#)

[Printer-friendly Version](#)

[Interactive Discussion](#)

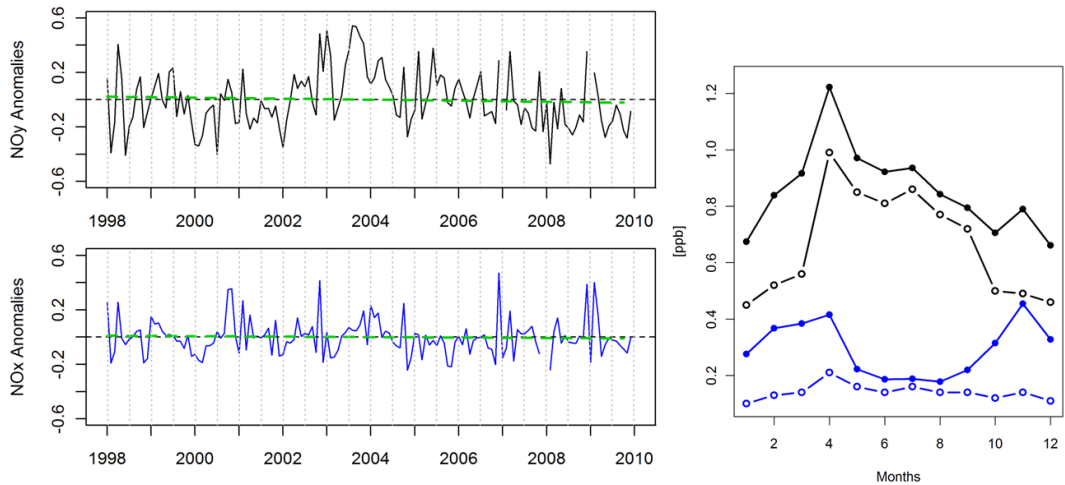


Fig. 5. Monthly anomalies of NO_y (black), NO_x (blue) from 1998–2009 with overall trend (green dashed lines represents linear trend). The mean (filled circles) and median (open circles) seasonal cycles for NO_y (black) and NO_x (blue) are additionally displayed in the small panel (right).

Long-term in situ measurements of NO_x and NO_y at Jungfraujoch

S. Pandey Deolal et al.

[Title Page](#)

[Abstract](#)

[Introduction](#)

[Conclusions](#)

[References](#)

[Tables](#)

[Figures](#)

◀

▶

◀

▶

[Back](#)

[Close](#)

[Full Screen / Esc](#)

[Printer-friendly Version](#)

[Interactive Discussion](#)

Long-term in situ measurements of NO_x and NO_y at Jungfraujoch

S. Pandey Deolal et al.

Figure 2 consists of three line graphs showing NO_x concentrations in ppb from 1998 to 2008 for three different locations. The y-axis for all graphs is 'NO_x [ppb]' ranging from 0 to 80. The x-axis is 'Years' from 1998 to 2008.

- Urban-suburban:** The y-axis ranges from 0 to 80 ppb. Data series include open circles (high), open squares (medium), and open triangles (low).
- Rural:** The y-axis ranges from 0 to 35 ppb. Data series include open circles (high), open squares (medium), and open triangles (low).
- Above 1000 m:** The y-axis ranges from 0 to 6 ppb. Data series include open circles (high), open squares (medium), and open triangles (low).

In all three locations, NO_x concentrations show a general downward trend over the period. The 'Urban-suburban' location shows the highest concentrations, followed by 'Rural', and then 'Above 1000 m' which shows the lowest concentrations.

Fig. 6. Annual averages of NO_x [ppb] at urban, rural and elevated sites from 1998–2009. Urban-suburban sites (black): Bern (open circles), Basel (filled circles), Zurich (open triangle), Dübendorf (filled squares), Lugano (crosses), Lausanne (open squares). Rural sites (green): Magadino (filled squares), Laegeren (filled circles), Taenikon (filled triangles), Payerne (open circles) and above 1000 m sites (blue): Chamount (open circle), Davos (filled squares), Rigi (filled triangles), Jungfraujoch (filled circles).

Title Page

Abstract

Introduction

Conclusions

References

Tables

Figures

1

A small, dark blue rectangular button with a white right-pointing triangle on the left side, indicating the next page or step in a sequence.

1

▶

1

1

Full Screen / Esc

ANSWER

Interactive Discussion

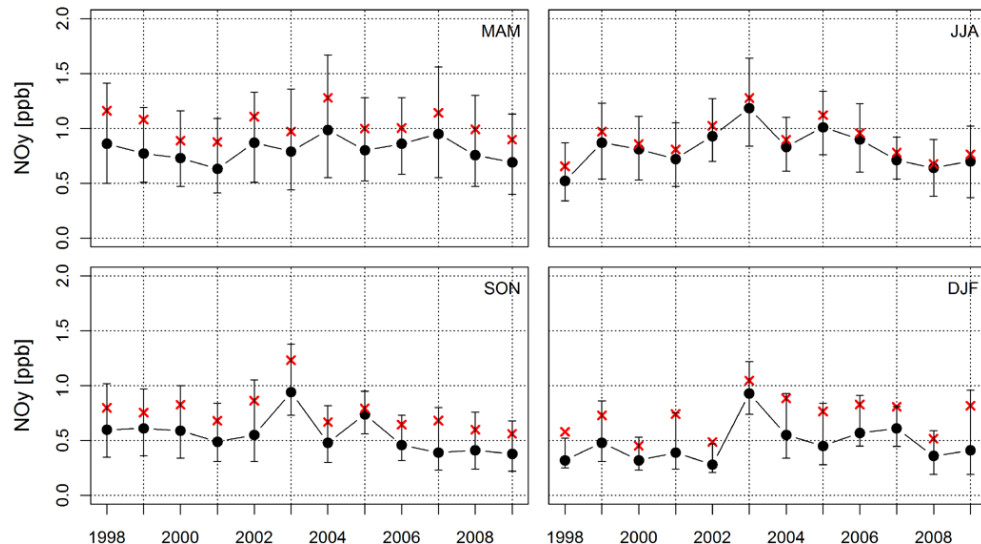


Fig. 7. Seasonal NO_y mean (red crosses), median (black round symbols), 25 % quantiles (lower vertical bar) and 75 % quantiles (upper vertical bar) from 1998–2009 for spring (MAM), summer (JJA), autumn (SON) and winter (DJF).

Long-term in situ measurements of NO_x and NO_y at Jungfraujoch

S. Pandey Deolal et al.

[Title Page](#)

[Abstract](#)

[Introduction](#)

[Conclusions](#)

[References](#)

[Tables](#)

[Figures](#)

◀

▶

◀

▶

[Back](#)

[Close](#)

[Full Screen / Esc](#)

[Printer-friendly Version](#)

[Interactive Discussion](#)

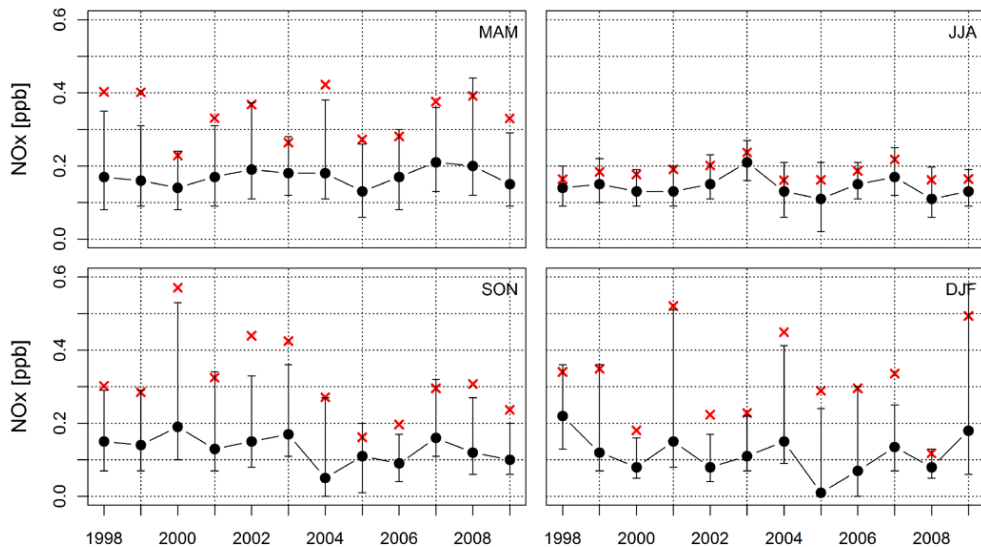


Fig. 8. Seasonal NO_x mean (red crosses), median (black round symbols), 25 % quantiles (lower vertical bar) and 75 % quantiles (upper vertical bar) from 1998–2009 for spring (MAM), summer (JJA), autumn (SON) and winter (DJF).

Long-term in situ measurements of NO_x and NO_y at Jungfraujoch

S. Pandey Deolal et al.

[Title Page](#)

[Abstract](#)

[Introduction](#)

[Conclusions](#)

[References](#)

[Tables](#)

[Figures](#)

◀

▶

◀

▶

[Back](#)

[Close](#)

[Full Screen / Esc](#)

[Printer-friendly Version](#)

[Interactive Discussion](#)

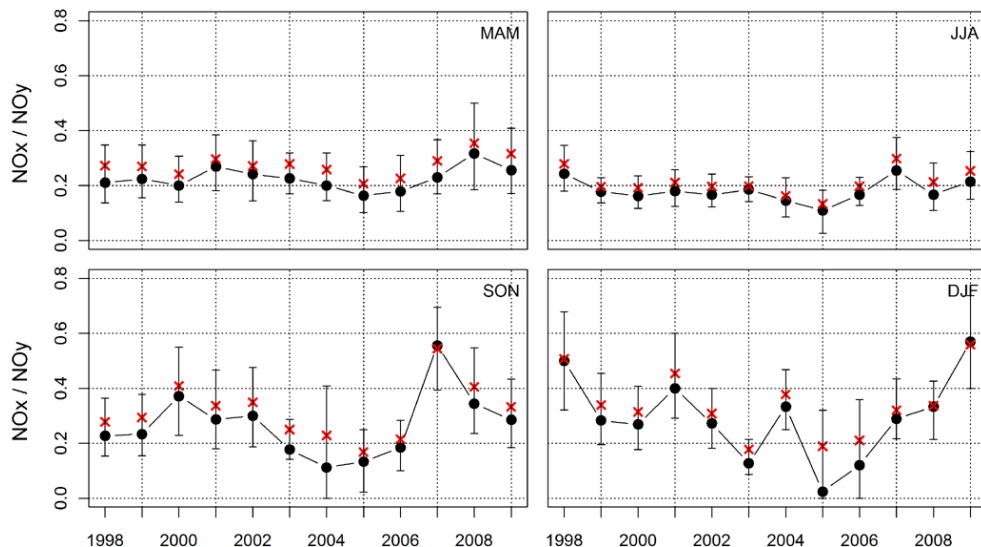


Fig. 9. Seasonal NO_x/NO_y mean (red crosses), median (black round symbols), 25 % quantiles (lower vertical bar) and 75 % quantiles (upper vertical bar) from 1998–2009 for spring (MAM), summer (JJA), autumn (SON) and winter (DJF).

Long-term in situ measurements of NO_x and NO_y at Jungfraujoch

S. Pandey Deolal et al.

[Title Page](#)

[Abstract](#)

[Introduction](#)

[Conclusions](#)

[References](#)

[Tables](#)

[Figures](#)

◀

▶

◀

▶

[Back](#)

[Close](#)

[Full Screen / Esc](#)

[Printer-friendly Version](#)

[Interactive Discussion](#)

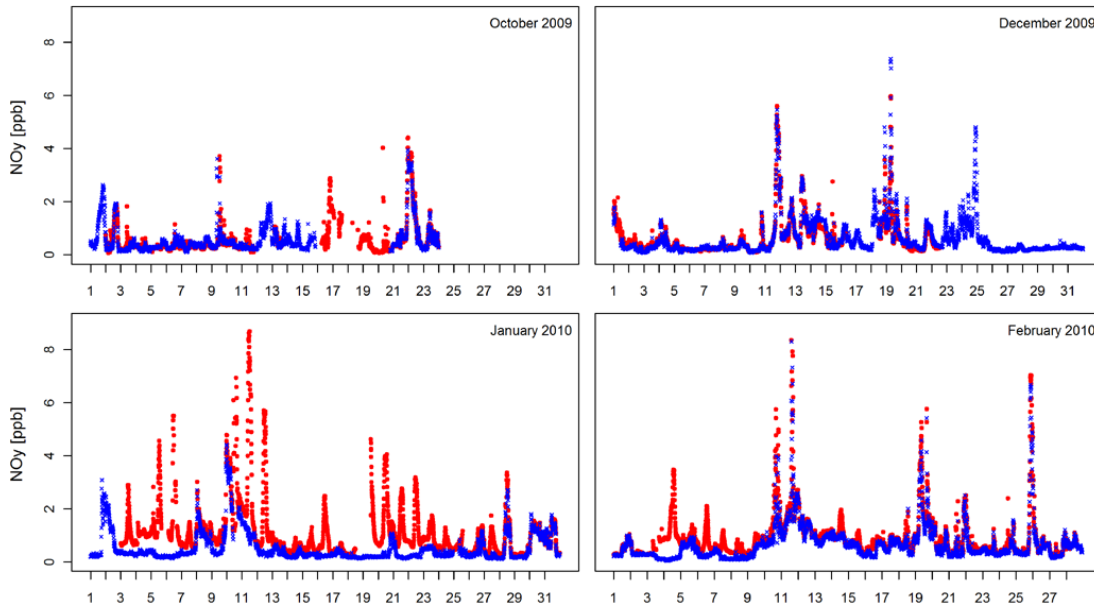


Fig. 10. Ten-minute averages of ETHZ NO_y (red) and Empa NO_y (blue) measurements in October/December 2009 and January/February 2010.

Long-term in situ measurements of NO_x and NO_y at Jungfraujoch

S. Pandey Deolal et al.

[Title Page](#)

[Abstract](#)

[Introduction](#)

[Conclusions](#)

[References](#)

[Tables](#)

[Figures](#)

◀

▶

◀

▶

[Back](#)

[Close](#)

[Full Screen / Esc](#)

[Printer-friendly Version](#)

[Interactive Discussion](#)

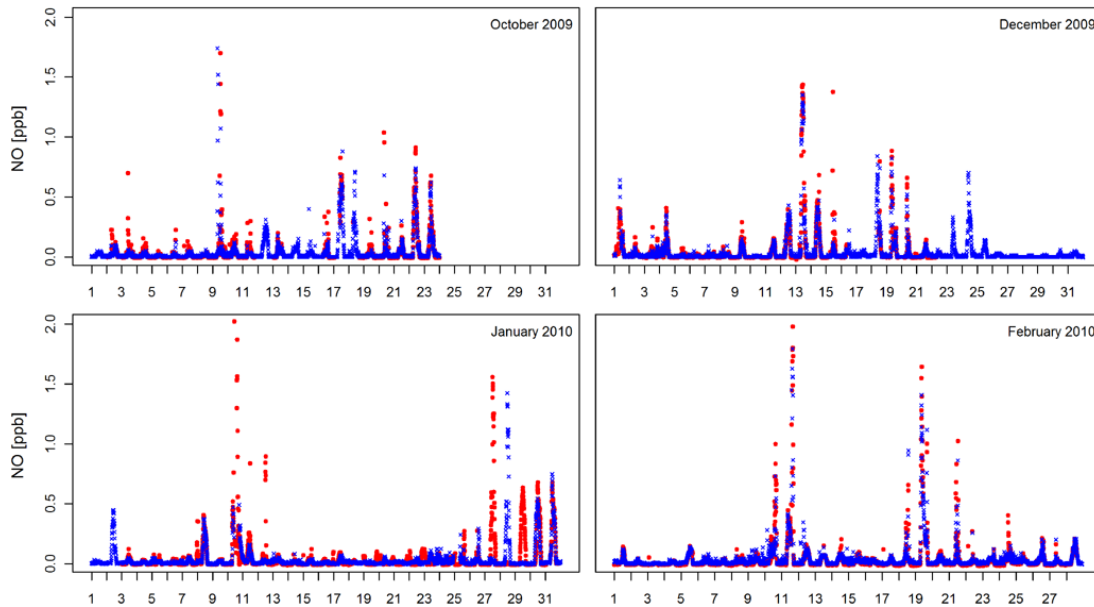


Fig. 11. Ten-minute averages of ETHZ NO (red) and Empa NO (blue) measurements in October/December 2009 and January/February 2010.

Long-term in situ measurements of NO_x and NO_y at Jungfraujoch

S. Pandey Deolal et al.

[Title Page](#)

[Abstract](#)

[Introduction](#)

[Conclusions](#)

[References](#)

[Tables](#)

[Figures](#)

◀

▶

◀

▶

[Back](#)

[Close](#)

[Full Screen / Esc](#)

[Printer-friendly Version](#)

[Interactive Discussion](#)

Long-term in situ measurements of NO_x and NO_y at Jungfraujoch

S. Pandey Deolal et al.

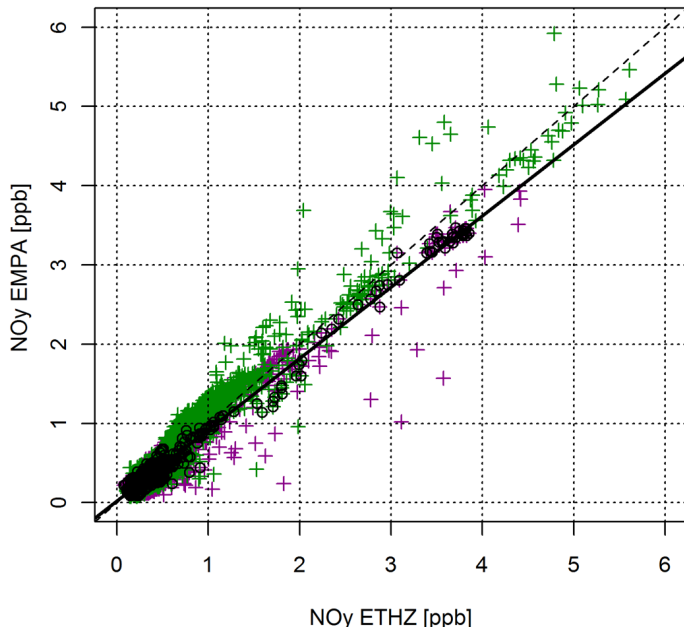


Fig. 12. Correlation between NO_y Empa and NO_y ETHZ ten minute averages in October (purple) and December (green). The dashed line represents one to one correspondence between data points and thick black line indicates linear fit to the filtered data (black).

- [Title Page](#)
- [Abstract](#) [Introduction](#)
- [Conclusions](#) [References](#)
- [Tables](#) [Figures](#)
- [◀](#) [▶](#)
- [◀](#) [▶](#)
- [Back](#) [Close](#)
- [Full Screen / Esc](#)
- [Printer-friendly Version](#)
- [Interactive Discussion](#)

Long-term in situ measurements of NO_x and NO_y at Jungfraujoch

S. Pandey Deolal et al.

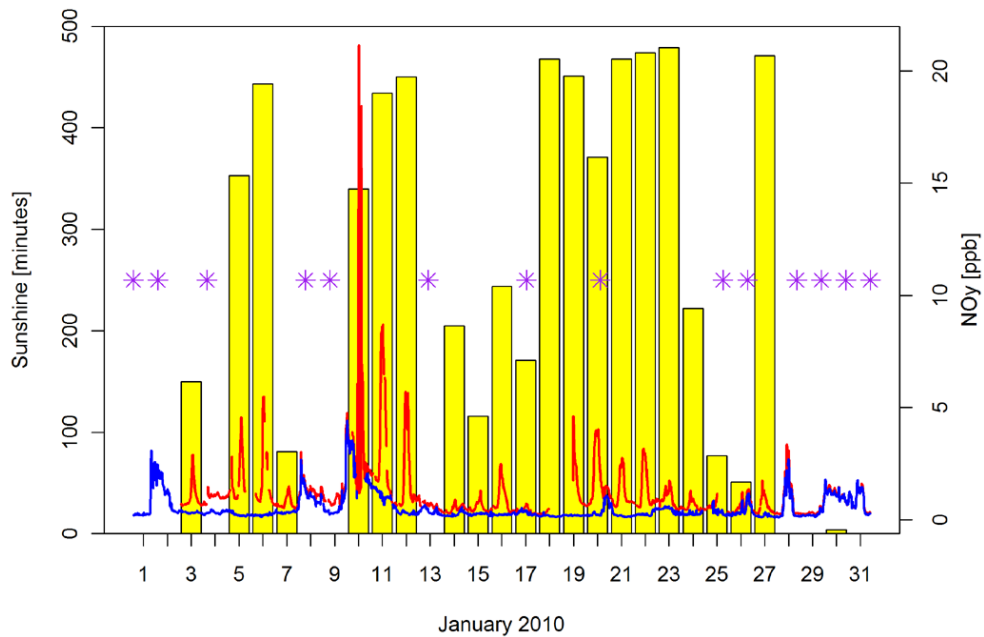


Fig. 13. Relationship of ETHZ NO_y (red line) and Empa NO_y (blue line) with sunshine and snowfall days in January (yellow bars: sunshine duration, purple stars: days with snowfall).

- [Title Page](#)
- [Abstract](#) [Introduction](#)
- [Conclusions](#) [References](#)
- [Tables](#) [Figures](#)
- [◀](#) [▶](#)
- [◀](#) [▶](#)
- [Back](#) [Close](#)
- [Full Screen / Esc](#)
- [Printer-friendly Version](#)
- [Interactive Discussion](#)

Long-term in situ measurements of NO_x and NO_y at Jungfraujoch

S. Pandey Deolal et al.

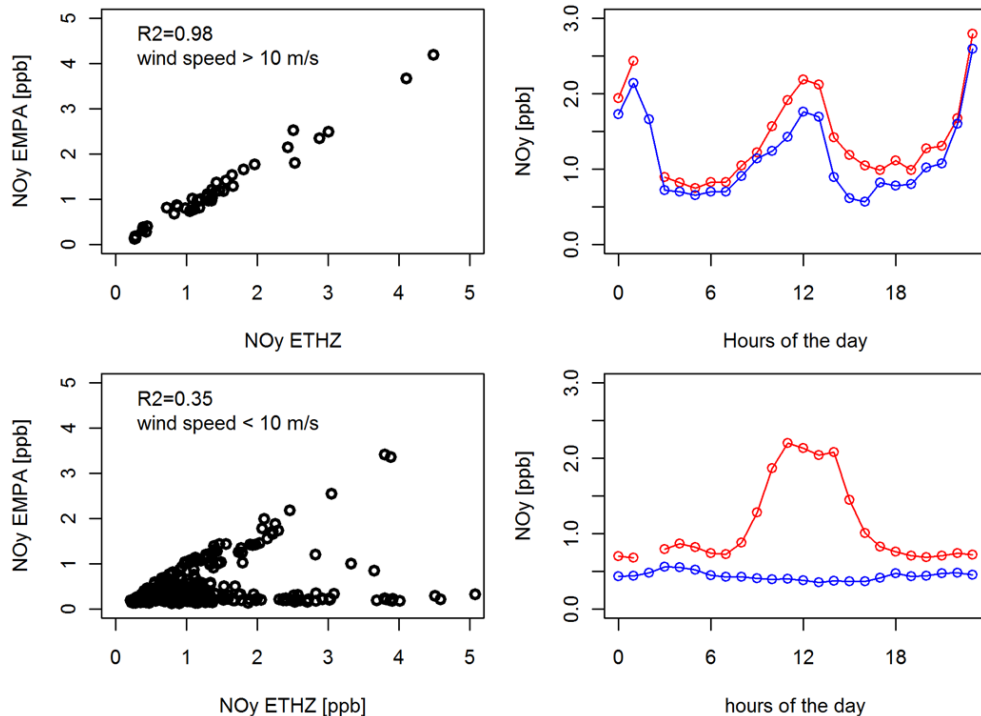


Fig. 14. Left panels: correlation between ETHZ NO_y and Empa NO_y in January for conditions with high wind speed (top) and low wind speed (bottom). Right panels: corresponding diurnal cycles of ETHZ NO_y (red) and Empa NO_y (blue) for situations with high and low wind speed, respectively.

- [Title Page](#)
- [Abstract](#) [Introduction](#)
- [Conclusions](#) [References](#)
- [Tables](#) [Figures](#)
- [◀](#) [▶](#)
- [◀](#) [▶](#)
- [Back](#) [Close](#)
- [Full Screen / Esc](#)
- [Printer-friendly Version](#)
- [Interactive Discussion](#)

Long-term in situ measurements of NO_x and NO_y at Jungfraujoch

S. Pandey Deolal et al.

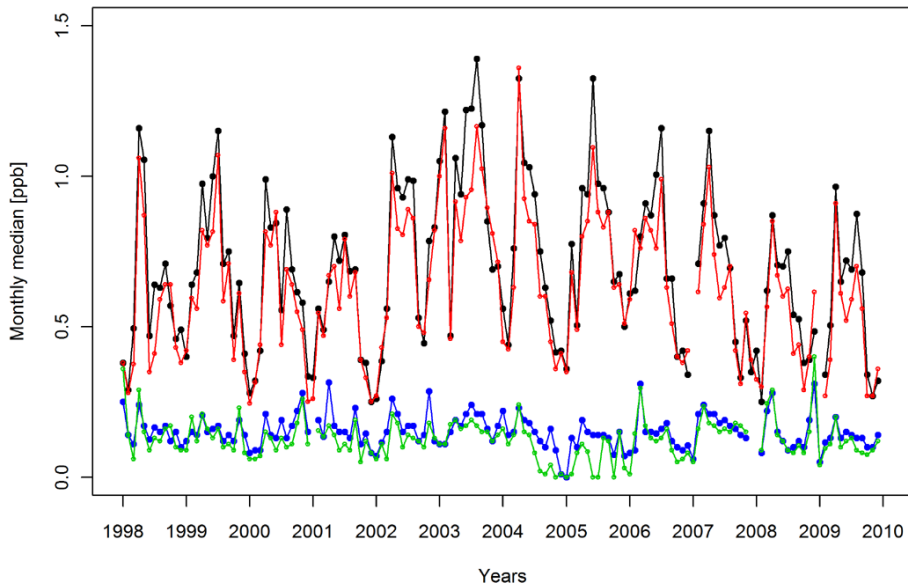


Fig. 15. Monthly median values of NO_y daytime (08:00–18:00 h local time, black) and NO_y nighttime (00:00–06:00 h local time, red), NO_x daytime (08:00–18:00 h local time, blue) and NO_x nighttime (00:00–06:00 h local time, green) from January 1998–December 2009.

[Title Page](#) [Abstract](#) [Introduction](#)
[Conclusions](#) [References](#)
[Tables](#) [Figures](#)

[◀](#) [▶](#)
[◀](#) [▶](#)
[Back](#) [Close](#)
[Full Screen / Esc](#)

[Printer-friendly Version](#)

[Interactive Discussion](#)